From February 2008 *High Frequency Electronics*

Power Combiners, Impedance Transformers and Directional Couplers: Part III

By Andrei Grebennikov

This multi-part article on coupler and combiner structures continues with an examination of microwave hybrids using various topologies

Microwave hybrids

The branch-line couplers or hybrids were firstly described more than six decades ago; however, the problem of their exact synthesis remained a puzzle for a number of years [53]. Initially, the branch-line hybrid was analyzed as a four-arm symmetrical network based on a superposition of the results obtained in the even and odd modes [54]. By writing the even and odd mode matrices together, the characteristic impedances of the branch lines and coupling into different ports can be obtained. A general synthesis procedure which can be applied to any structure of a multibranch hybrid, based on an invariance of the Richard's variable $S = j\tan\theta$ to the transformation of $S \rightarrow 1/S$ apart from a 180° phase change, had become available a decade later [55]. As a result, with highly precise computer-design techniques available for branch-line hybrids, it became possible to generate any coupling value in the useful 0 to 15 dB coupling range. Waveguide designs which have been used in large complex feeds for phase-array radars, are compact, highly predictable in amplitude and phase characteristics, and handle very high power. Coaxial, microstrip or stripline implementations of branch-line hybrids provide simple planar structures of moderate bandwidth capability, up to about 2/3 of an octave.

For a fully matched case with standard 50-Ω source and load impedances, when the characteristic impedances of its transverse branches are 50 Ω and the characteristic impedances of its longitudinal main lines are

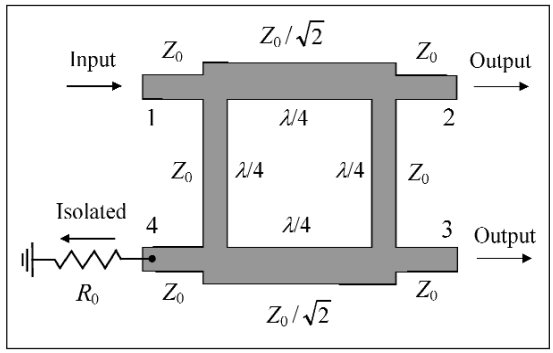

Figure 30 · Microstrip branch-line quadrature hybrid.

$$50/\sqrt{2} = 35.4\Omega$$

the microstrip branch-line hybrid shown in Fig. 30 represents a 3-dB directional coupler, for which power in arm 1 divides evenly between arms 2 and 3 with the phase shift of 90°. No power is delivered to arm 4, because the signal flowing through different paths (lengths of λ/4 and 3λ/4) have the same amplitude and opposite phases at this port. The branch-line hybrid does not depend on the load mismatch level for equal reflected coefficients from the outputs when all reflected power is dissipated in the 50-Ω ballast resistor. However, in practice, due to the quarter-wavelength transmission-line requirement, the bandwidth of such a single-stage quadrature branch-line hybrid is limited to 10-20%.

Figure 31 shows the calculated frequency bandwidth characteristics of a single-section branch-line hybrid matched at the center bandwidth frequency with the load impedance $Z_L = Z_0 = 50\ \Omega$, where C_{12} is the insertion loss calculated as the ratio of powers at the input

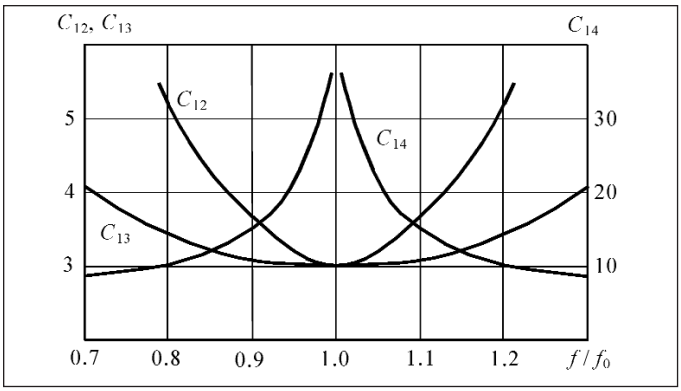

Figure 31 · Bandwidth performance of the single-section branch-line hybrid.

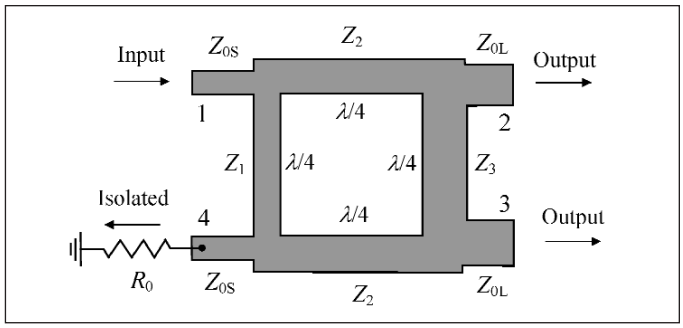

Figure 32 · Microstrip branch-line quadrature impedance-transforming hybrid.

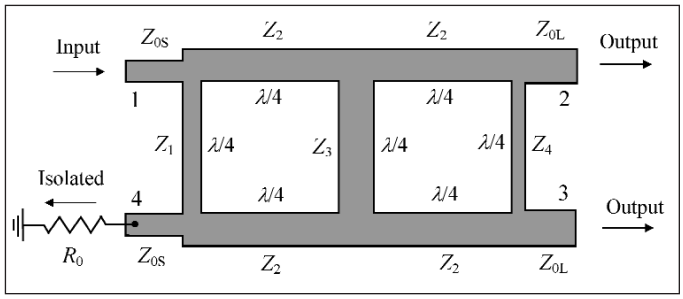

Figure 33 · Broadband microwave branch-line quadrature hybrid.

port 1 relative the output port 2, C_{13} is the coupling calculated as the ratio of powers at the input port 1 relative to the output port 3, and C_{14} is the isolation calculated as the ratio of powers at the input port 1 relative to the isolated port 4 [56]. At millimeter-wave frequencies, the lengths of the microstrip lines can actually get shorter than the widths and the mutual coupling between the input lines and discontinuities at the input increases significantly. This has a direct effect on the input/output match, frequency bandwidth and isolation. To minimize the effect of these problems, the branch-line hybrid can be designed as a two-section hybrid using three-quarterwave lines for the series main lines and quarterwave lines for the shunt branch lines, with all inputs/outputs orthogonal to each other [57]. As a result, the return loss is 10 dB or better over 90% of the band, the isolation can achieve 10 dB or better over the whole band, and the difference in the coupling can be equal or less than 1 dB over about 75% of the frequency band from 26 to 40 GHz.

If one pair of terminating resistors has different values compared to the other pair, the resulting branch-line hybrid can operate as a directional coupler and an impedance transformer simultaneously [58]. Design values of the branch- and main-line characteristic impedances for a single-section branch-line hybrid shown in Fig. 32, related to the input source impedance Z_{0S} and output load impedance Z_{0L}, can be calculated by

$$Z_1 = \frac{Z_{0S}}{K} \tag{28}$$

$$Z_2 = \sqrt{\frac{Z_{0S}Z_{0L}}{1+K^2}} \tag{29}$$

$$Z_3 = \frac{Z_1 Z_{0L}}{Z_{0S}} \tag{30}$$

where K is the voltage-split ratio between output ports 2 and 3, and $R_0 = Z_{0S}$ [59]. Such a hybrid with a 2-to-1 (50- to 25-Ω) impedance transformation ratio can provide approximately 20-percent frequency bandwidth with ±0.25 dB amplitude imbalance. However, for a fixed directivity, the frequency bandwidth of branch-line impedance-transforming hybrid increases as the output-to-input impedance ratio is reduced [58].

The operating bandwidth can be significantly increased using multi-stage impedance-transforming hybrids. A two-section branch-line impedance-transforming quadrature hybrid is shown in Fig. 33. To design this hybrid with the given impedance transformation ratio r and power-split ratio K^2, the branch- and main-line characteristic impedances should be chosen according to

$$Z_1 = Z_{0S}\sqrt{r\frac{t^2-r}{t-r}} \tag{31}$$

$$\frac{Z_2^2}{Z_3} = Z_{0S}\sqrt{r-\left(\frac{r}{t}\right)^2} \tag{32}$$

$$Z_4 = Z_{0S}\frac{\sqrt{r\left(t^2-r\right)}}{t-1} \tag{33}$$

where [60],

$$t = 4\sqrt{1+K^2}$$

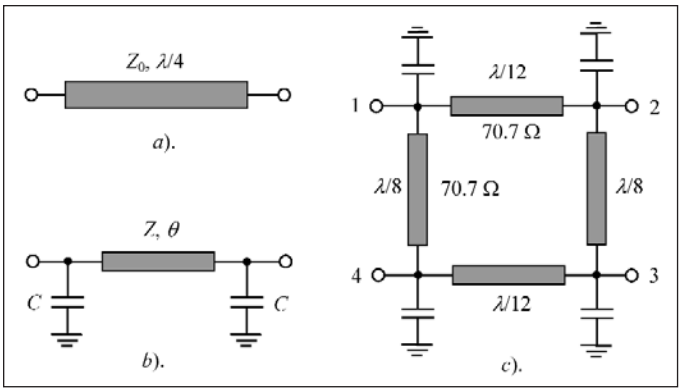

Figure 34 · Reduced-size branch-line quadrature hybrid.

The condition of $Z_2 = Z_3$ gives maximum bandwidth when the best performance at the center bandwidth frequency is specified.

For an equal power division when $K = 1$, the condition $t = r\sqrt{2}$ specifies a minimum value of r which is equal to 0.5. However, in practice, it is better to choose r in the range of 0.7 to 1.3, in order to provide the physically realizable branch-line characteristic impedances for 50-Ω input impedance. For example, for the 50 to 35 Ω impedance transformation using a two-stage hybrid, the impedances are as follows: $Z_1 = 72.5$ Ω, $Z_2 = Z_3 = 29.6$ Ω, and $Z_4 = 191.25$ Ω. This gives the power balance between the output ports better than 0.5 dB with the return loss and isolation better than 20 dB over a frequency bandwidth of 25% for a 2-GHz hybrid.

For monolithic microwave integrated circuit (MMIC) applications, the overall size of the quadrature branch-line hybrids with quarterwave transmission lines is too large. Therefore, it is attractive to replace each quarterwave branch line with the combination of a short-length transmission line and two shunt capacitors providing the same bandwidth properties. Consider the admittance matrix $[Y_a]$ for a quarterwave transmission line shown in Fig. 34(a) and the admittance matrix $[Y_b]$ for a circuit consisting of a short transmission line with two shunt capacitors shown in Fig. 34(b) which are given by

$$[Y_a] = \frac{1}{jZ_0}\begin{bmatrix} 0 & -1 \\ -1 & 0 \end{bmatrix} \tag{34}$$

$$[Y_b] = \frac{1}{jZ\sin\theta}\begin{matrix} \cos\theta - \omega CZ\sin\theta & -1 \\ -1 & \cos\theta - \omega CZ\sin\theta \end{matrix} \tag{35}$$

where Z_0 is the characteristic impedance of a quarterwave line, Z and θ are the characteristic impedance and electrical length of a shortened line, and C is the shunt capacitance. By equating the corresponding Y-parameters in Eqs. (34) and (35), the simple ratios between the circuit

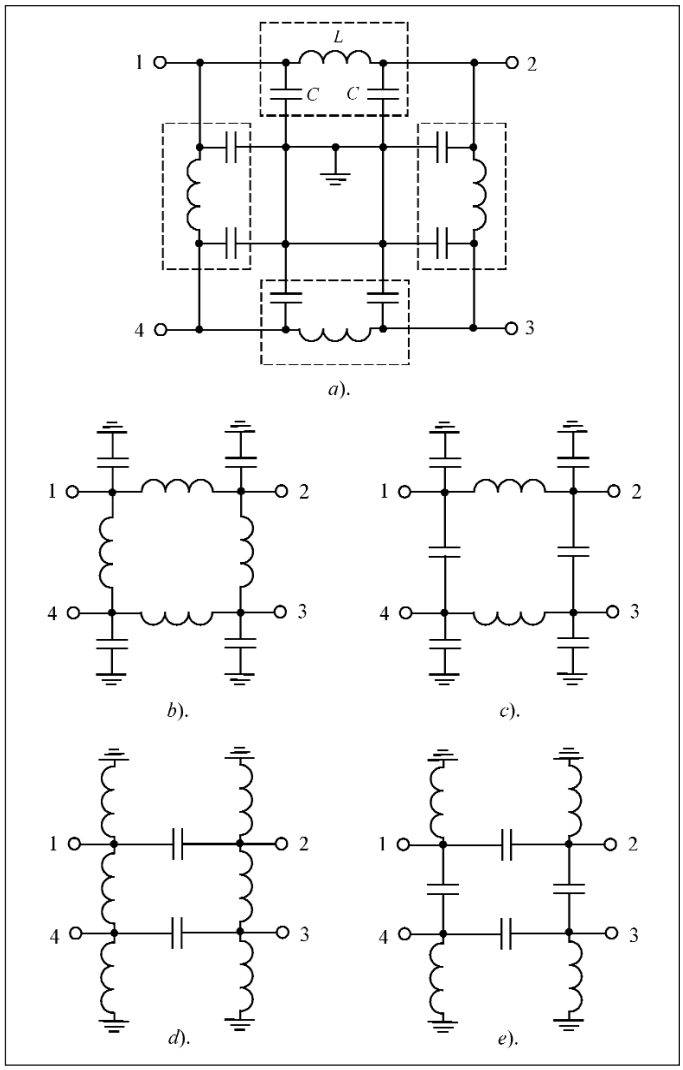

Figure 35 · Equivalent circuits of lumped LC-type hybrid.

parameters can be obtained in the form of

$$Z = \frac{Z_0}{\sin\theta} \tag{36}$$

$$C = \frac{1}{\omega Z_0 \cos\theta} \tag{37}$$

from which it follows that the lengths of the hybrid transmission lines can be made much shorter by increasing their characteristic impedance Z. For example, when choosing the electrical length of $\theta = 45°$, the characteristic impedance of the transmission line increases by a factor of $\sqrt{2}$.

A circuit schematic of the reduced-size branch-line quadrature hybrid is shown in Fig. 34(c) [61]. Compared

to the conventional branch-line hybrid with characteristic impedances of its branch- and main-lines of Z_0 and $Z_0/\sqrt{2}$ respectively, the circuit parameters of the reduced-size branch-line hybrid are obtained from

$$\theta_1 = \sin^{-1}\left(\frac{Z_0}{Z}\right) \qquad (38)$$

$$\theta_2 = \sin^{-1}\left(\frac{Z_0}{Z\sqrt{2}}\right) \qquad (39)$$

$$\omega C Z_0 = \sqrt{1-\left(\frac{Z_0}{Z}\right)^2} + \sqrt{2-\left(\frac{Z_0}{Z}\right)^2}$$

(eq. 40), where θ_1 and θ_2 are the electrical lengths of the shunt branch-line and series main-line, respectively. For a particular case of the standard characteristic impedance Z_0 = 50 Ω, the characteristic impedance and electrical lengths of the transmission lines are defined as

$$Z = Z_0 / \sqrt{2}$$

$$\theta_1 = 45°$$

$$\theta_2 = 30°$$

as shown in Fig. 34(c). Experimental results for a 25-GHz reduced-size branch-line quadrature hybrid show that its bandwidth performance is slightly narrower than that of the conventional quarterwave hybrid, but its overall size is more than 80% smaller.

To further reduce the MMIC size, the transmission lines can be fully replaced by the lumped planar inductors. Such an approach becomes possible because the symmetrical lumped *LC*-type π- or *T*-section is equivalent at a single frequency to the transmission-line section with the appropriate characteristic impedance and electrical length. The lumped-element equivalent circuit of a transmission-line branch-line hybrid is shown in Fig. 35(a) [62]. This circuit has also some additional advantages when each its section can work as a separate impedance transformer, a low-pass filter, and a phase shifter. The circuit can be diced into four separate sections and cascaded for the desired transmission characteristics. The circuit analysis indicates that various types of networks fulfill the conditions required for an ideal hybrid. Therefore, greater design flexibility in the choice of the hybrid structure and performance is possible. Several possible single-section two-branch hybrid options are shown in Fig. 35 [63]. In this case, it should be noted that not only a low-pass section but also a high-pass section can be

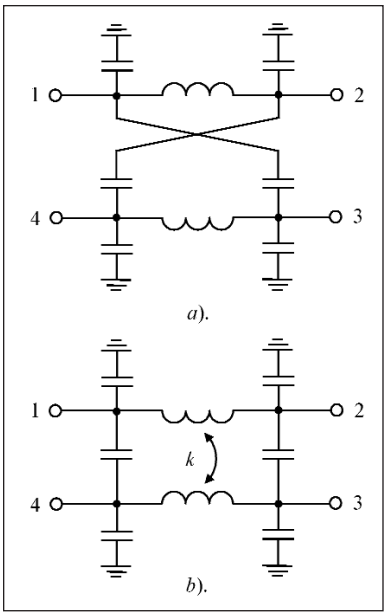

Figure 36 · Equivalent circuits of lumped hybrid with capacitive and inductive coupling.

respectively used. In the latter case, the high-pass *LC* section is considered an equivalent single-frequency replacement for a 270-degree transmission line [64]. Figures 35(c) and 35(d) illustrate the use of both low-pass and high-pass sections simultaneously, while only high-pass sections compose the hybrid shown in Fig. 35(e). The performances of the hybrids shown in Figs. 35(b) and 35(e) are very similar to that of the classical single-section branch-line hybrid. The bandwidth performances of the hybrids shown in Figs. 35(c) and 35(d) are narrower because the power balance between their output ports is much narrower. Broader bandwidth and lower output impedances can be provided with a two-section three-branch lumped-element hybrid.

Figure 36(a) shows the equivalent circuit of a capacitively coupled lumped-element hybrid, which is used for monolithic design of variable phase shifters [65]. However, the power and phase balance bandwidth at the output ports of this hybrid is very narrow, in the limits of a few percent. An alternative design of an inductively coupled lumped-element hybrid is shown in Fig. 36(b) [66]. As a basic element, it includes lumped multiturn mutually coupled spiral inductors with the coupling coefficient, which can be realized using a bifilar (a sandwich of two multiturn spiral inductors with inner and outer windings) spiral transformer to achieve a coupling coefficient $k = 0.707$. In this case, this basic lumped-element configuration is completely equivalent to a transmission line in the vicinity of the center bandwidth frequency. The inductively coupled hybrid can provide a power balance within 0.2 dB and phase balance within 1° in a frequency bandwidth of ±10% in 2-GHz wireless applications. However, during the design procedure, some parasitic effects should be taken into account. For example, the coupled inductor itself has a significant value of internal capacitance. Also, the finite value of the inductor quality factor results in a modest amplitude imbalance, but leads to a significant phase deviation from ideal quadrature 90-degree difference. In this case, to compensate for the resulting performance degradation, the electromagnetic simulation of the

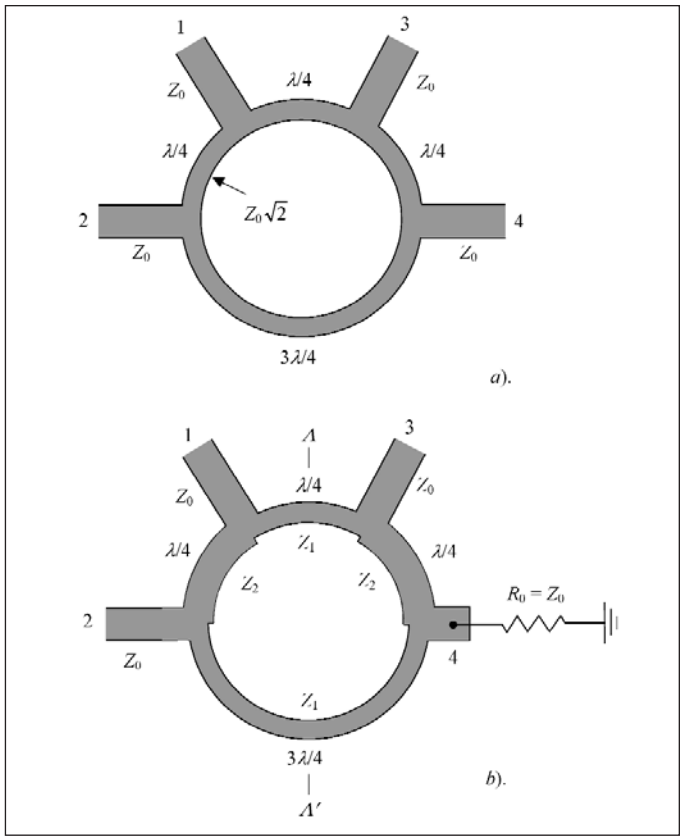

Figure 37 · Microstrip rat-race ring hybrids.

structure and optimization of the values of the added shunt capacitors on both sides of the circuit are required. Two of these inductively-coupled hybrids can be cascaded in tandem to significantly extend the frequency bandwidth. As a result, the phase shift of 93 ±6°, the insertion loss between 1 and 1.5 dB, the return loss better than 16 dB, and the isolation between the output ports better than 18 dB were measured over the frequency range from 2 to 6 GHz [66].

A hybrid-ring directional coupler or rat-race, which is one of the fundamental components used in microwave circuits was described and analyzed more than six decades ago [67]. Its operation principle is based on an assumption that the voltage at any point along the transmission line is a superposition of the forward and backward propagating waves. Signal from the excitation source spreads out in the driving point and propagates along the line. As the forward wave reaches the far-end termination, it reflects, propagates backward, reflects from the near-end termination, propagates forward again, and continues in a loop. According to this wave behavior, a pure standing wave is set up within the ring when there is no mechanism for dissipation other than the minor ohmic losses associated with wave transmission. The point of voltage minimum (zero) corresponds to the case

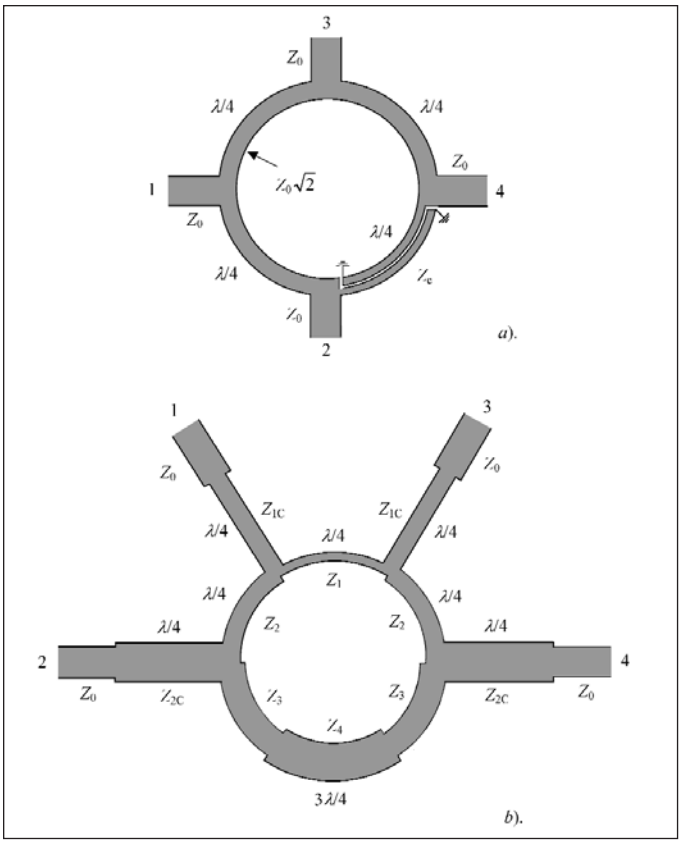

Figure 38 · Microstrip broadband ring hybrids.

when the waves have phase shift of 180 degrees with respect to each other. As a result, the standing wave within the ring can be mapped by marking off alternate voltage maxima and minima at quarterwave intervals. Consequently, if standing waves are set up in the main arm, the side arm receives maximum power when a voltage minimum of the standing-wave pattern coincides with the center of this arm and minimum power when a voltage maximum located in this point.

The $3\lambda/2$ ring hybrid, which microstrip topology is shown in Fig. 37(a), can be used to divide the driving power or to combine the powers from two sources. In the case of power division, a signal applied to the port 1 will be evenly split into two in-phase components at ports 2 and 3, and port 4 will be isolated. If the input signal is applied at port 4, it will be equally split into two components with 180-degree difference at ports 2 and 3, and port 1 will be isolated. When operated as a combiner, with input signals applied at ports 2 and 3, the sum of the input signals will be delivered to port 1. Their difference will flow to port 4 and dissipated in corresponding ballast resistor R_0. For equal signals and matched ring hybrid with $Z_0 = R_0$, there is zero-power dissipation at port 4 [54].The ideal rat-race or ring hybrid has the bandwidth of approximately 27.6% at the tolerance limits of the deviation of 0.43 dB for split and of 20 dB for the maximum return loss and isolation.

Generally, a hybrid-ring directional coupler can provide arbitrary power divisions when the power-split ratio is adjusted by varying the impedances between the arms [68]. Figure 37(b) shows the planar microstrip topology of a ring hybrid where the characteristic impedances of four arms are equal to the standard characteristic impedance Z_0. The variable parameters are the two characteristic impedances Z_1 and Z_2, which determine the degree of coupling of the output arms and the impedance matching condition for the input arm. The analysis of this ring hybrid consists of the usual procedure of reducing the four-terminal network to a two-terminal network by taking advantage of the symmetry about the plane *A-A′*. For example, when two in-phase waves of equal amplitude are applied to terminals 2 and 3, the current is zero at the plane *A-A′*. As a result, the ring can be open-circuited at this plane and only one half of the circuit can be analyzed. This condition is called the even mode. On the other hand, the odd-mode condition is a result of applying the opposite-phase waves of equal amplitude to terminals 2 and 3 when the voltage at plane *A-A′* is zero. In this case, the ring can be short-circuited at this plane and only one half of the circuit can be analyzed. Once the scattering matrices for the even and odd modes are known, the reflected waves in each arm can be determined. Then, by superimposing the waves of the two modes, the resultant reflected waves in each arm and a single incident wave in one arm is obtained. Thus, if arm 1 is input, the output voltage ratio between arm 2 and 3 is equal to Z_1/Z_2, and no power is delivered to the isolated port 4 where the ballast resistor $R_0 = Z_0$ is connected.

Although usually considered a narrow-band device, the rat-race hybrid can provide much broader performance if its three-quarter wavelength section (a main limiting factor in a conventional configuration) is replaced by one having the same characteristic impedance, but whose electrical length is realized by a quarter wavelength line that is also an ideal phase-reversing network [69], which may be a coaxial cable with a crossover of its inner and outer conductors at one end, The result is an isolation of more than 20 dB in a frequency bandwidth of 30 percent [56]. As a compact planar alternative, a pair of equilateral broadside-coupled segments of strip transmission lines having diametrically opposing ends short-circuited (Fig. 38(a)) approximates a phase-reversing network over a wide frequency range.

The characteristic impedance of the coupled section Z_c is given by

$$Z_c = \frac{2Z_{0e}Z_{0o}\sin\theta}{\sqrt{(Z_{0e}-Z_{0o})^2-(Z_{0e}-Z_{0o})^2\cos^2\theta}} \qquad (41)$$

where Z_{0e} is the even-mode impedance, Z_{0o} is the odd-mode impedance, and θ is the electrical length of the coupled region [70]. To realize a required 270 degree of phase shift, θ must be 90 degree, resulting in

$$Z_c = \frac{2Z_{0e}Z_{0o}}{Z_{0e} - Z_{0o}} \tag{42}$$

which for proper operation should be equal at midband to $Z_0\sqrt{2}$. Since $Z_0 = \sqrt{Z_{0e}Z_{0o}}$ then,

$$Z_{0e} = \left(2 + \sqrt{2}\right)Z_0 \tag{43}$$

$$Z_{0o} = \left(2 - \sqrt{2}\right)Z_0 \tag{44}$$

which means that, for a 50-Ω transmission system and a median 3-dB coupling, Z_{0e} must be 170.7 Ω and Z_{0o} must be 29.3 Ω.

To extend the frequency bandwidth and simplify fabrication process with a uniplanar structure, the ring hybrid can represent a slotline ring with one slotline and three coplanar waveguide arms [71]. The design technique substitutes one reverse-phase slotline *T*-junction for the conventional rat-race phase delay section. Since the phase reverse of the slotline *T*-junction is frequency independent, the resulting slotline ring hybrid provides a broad bandwidth. Experimental results show that this uniplanar crossover ring-hybrid coupler has a bandwidth from 2 to 4 GHz with ±0.4 dB power dividing balance and ±1° phase balance. By using a micro-coplanar stripline ring with a broadband coplanar stripline phase inverter and four coplanar waveguide arms, the coupling between the output ports is within 3.5 ±0.5 dB over the frequency range from 1.43 to 2.95 GHz [72].

However, it is possible to increase the operating bandwidth of the conventional rat-race without a quarterwave phase-reversing section by applying the concept of hypothetical ports and adding the proper quarterwave transformer to each port [73]. The bandwidth will be significantly broadened by replacing a three-quarterwave equal-impedance section with symmetrical transmission-line structure, the middle quarterwave section of which has different characteristic impedance. To optimally realize this, the numerical optimization procedure to minimize an objective evaluation function is required. In this case, to improve coupling, matching and isolation, it is necessary to connect either the open-circuited compensating stubs at the hypothetical ports (connecting points of the quarterwave lines with different characteristic impedances), or to add the quarterwave transformers (transmission lines with different characteristic impedances) to the hybrid ports, as shown in Fig. 38(b). As a result, the frequency bandwidth of the improved ring hybrid becomes 1.84 times as wide as the conventional rat-race.

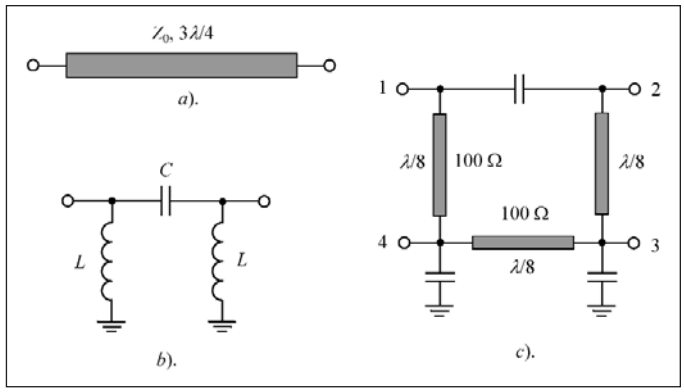

Figure 39 · Reduced-size ring hybrid.

To significantly reduce the overall size of the conventional ring hybrid with the 90-degree and 270-degree transmission line sections which is crucial for MMIC design, the principle of a single-frequency equivalence between the circuits with lumped and distributed parameters can be applied [64]. Let us compare the elements of the transmission matrix [*ABCD*a] for a 270-degree transmission line and the transmission matrix [*ABCD*b] for a high-pass π-type lumped circuit, consisting of the series capacitors and two shunt inductors, given by

$$[ABCD_a] = \begin{bmatrix} \cos\theta & jZ_0\sin\theta \\ j\dfrac{\sin\theta}{Z_0} & \cos\theta \end{bmatrix}\Bigg|_{\theta=3\pi/2} = \begin{bmatrix} 0 & -jZ_0 \\ \dfrac{-j}{Z_0} & 0 \end{bmatrix} \tag{45}$$

$$[ABCD_b] = \begin{bmatrix} 1 & 0 \\ -j/\omega L & 1 \end{bmatrix}\begin{bmatrix} 1 & -j/\omega C \\ 0 & 1 \end{bmatrix}\begin{bmatrix} 1 & 0 \\ -j/\omega L & 1 \end{bmatrix}$$

$$= \begin{bmatrix} 1 - \dfrac{1}{\omega^2 LC} & -j\dfrac{1}{\omega C} \\ -j\dfrac{1}{\omega L}\left(2 - \dfrac{1}{\omega^2 LC}\right) & 1 - \dfrac{1}{\omega^2 LC} \end{bmatrix} \tag{46}$$

Equating the corresponding elements of both matrices yields the simple expressions to determine the circuit elements in the form of

$$Z_0\omega C = \frac{Z_0}{\omega L} = 1 \tag{47}$$

Hence, to reduce the size of a ring hybrid, a 270-degree transmission line shown in Fig. 39(a) is replaced by a high-pass lumped section. Then, the three quarterwave-line sections are replaced by shortened ones with two shunt capacitors shown in Fig. 34(b) for a branch-line coupler. Finally, the characteristic impedance of the transmission line sections is chosen so that the shunt inductors

of the high-pass section shown in Fig. 39(b) could resonant with the shunt capacitors of the low-pass section at the center bandwidth frequency, in order to completely remove these components. Figure 39(c) shows the circuit diagram of the reduced-size ring hybrid with the characteristic impedances of the transmission-line sections of 100 Ω and their electrical lengths of 45 degree [61]. As a result, the overall reduced hybrid size is more than 80 percent smaller than that of the conventional hybrid.

This article series will conclude next month. The final topic is coupled-line directional couplers.

References

53. S. B. Cohn and R. Levy, "History of Microwave Passive Components with Particular Attention to Directional Couplers," *IEEE Trans. Microwave Theory Tech.,* vol. MTT-32, pp. 1046-1054, Sept. 1984.

54. J. Reed and G. J. Wheeler, "A Method of Analysis of Symmetrical Four-Port Networks," *IRE Trans. Microwave Theory Tech.,* vol. MTT-4, pp. 246-252, Oct. 1956.

55. R. Levy and L. Lind, "Synthesis of Symmetrical Branch-Guide Directional Couplers," *IEEE Trans. Microwave Theory Tech.,* vol. MTT-16, pp. 80-89, Feb. 1968.

56. A. Grebennikov, *RF and Microwave Power Amplifier Design,* New York: McGraw-Hill, 2004.

57. P. Meaney, "A Novel Branch-Line Coupler Design for Millimeter-Wave Applications," *1990 IEEE MTT-S Int. Microwave Symp. Dig.,* pp. 585-588.

58. L. F. Lind, "Synthesis of Asymmetrical Branch-Guide Directional Coupler-Impedance Transformers," *IEEE Trans. Microwave Theory Tech.,* vol. MTT-17, pp. 45-48, Jan. 1969.

59. R. K. Gupta, S. E. Anderson, and W. J. Getsinger, "Impedance-Transforming 3-dB 90° Hybrids," *IEEE Trans. Microwave Theory Tech.,* vol. MTT-35, pp. 1303-1307, Dec. 1987.

60. S. Kumar, C. Tannous, and T. Danshin, "A Multisection Broadband Impedance Transforming Branch-Line Hybrid," *IEEE Trans. Microwave Theory Tech.,* vol. MTT-43, pp. 2517-2523, Nov. 1995.

61. T. Hirota, A. Minakawa, and M. Muraguchi, "Reduced-Size Branch-Line and Rat-Race Hybrid for Uniplanar MMIC's," *IEEE Trans. Microwave Theory Tech.,* vol. MTT-38, pp. 270-275, March 1990.

62. M. Caulton, B. Hershenov, S.P. Knight, and R. E. DeBrecht, "Status of Lumped Elements in Microwave Integrated Circuits - Present and Future," *IEEE Trans. Microwave Theory Tech.,* vol. MTT-19, pp. 588-599, July 1971.

63. R. W. Vogel, "Analysis and Design of Lumped- and Lumped-Distributed-Element Directional Couplers for MIC and MMIC Applications," *IEEE Trans. Microwave Theory Tech.,* vol. MTT-40, pp. 253-262, Feb. 1992.

64. S. J. Parisi, "180° Lumped Element Hybrid," *1989 IEEE MTT-S Int. Microwave Symp. Dig.,* pp. 1243-1246.

65. R. C. Frye, S. Kapur and R. C. Melville, "A 2-GHz Quadrature Hybrid Implemented in CMOS Technology," *IEEE J. Solid-State Circuits,* vol. SC-38, pp. 550-555, March 2003.

66. F. Ali and A. Podell, "A Wide-Band GaAs Monolithic Spiral Quadrature Hybrid and its Circuit Applications," *IEEE J. Solid-State Circuits,* vol. SC-26, pp. 1394-1398, Oct. 1991.

67. W. A. Tyrrell, "Hybrid Circuits for Microwaves," *Proc. IRE,* vol. 35, pp. 1294-1306, Nov. 1947.

68. C. Y. Pon, "Hybrid-Ring Directional Coupler for Arbitrary Power Divisions," *IRE Trans. Microwave Theory Tech.,* vol. MTT-9, pp. 529-535, Nov. 1961.

69. S. March, "A Wideband Stripline Hybrid Ring," *IEEE Trans. Microwave Theory Tech.,* vol. MTT-16, pp. 361, June 1968.

70. G. L. Matthaei, E. M. T. Jones, and L. Young, *Microwave Filters, Impedance-Matching Networks and Coupling Structures,* New York: Artech House, 1980.

71. C.-H. Ho, L. Fan, and K. Chang, "Broad-Band Uniplanar Hybrid-Ring and Branch-Line Couplers," *IEEE Trans. Microwave Theory Tech.,* vol. MTT-41, pp. 2116-2124, Dec. 1993.

72. T. Wang and K. Wu, "Size-Reduction and band-Broadening Design Technique of Uniplanar Hybrid Ring Coupler Using Phase Inverter for M(H)MIC's," *IEEE Trans. Microwave Theory Tech.,* vol. MTT-42, pp. 198-206, Feb. 1999.

73. D. I. Kim and Y. Naito, "Broad-Band Design of Improved Hybrid-Ring 3-dB Directional Couplers," *IEEE Trans. Microwave Theory Tech.,* vol. MTT-30, pp. 2040-2046, Nov. 1982.

Author Information

Andrei Grebennikov received his Dipl. Ing. degree in radio electronics from Moscow Institute of Physics and Technology and PhD degree in radio engineering from Moscow Technical University of Communications and Informatics in 1980 and 1991, respectively. He has extensive academic and industrial experience working with Moscow Technical University of Communications and Informatics, Russia, Institute of Microelectronics, Singapore, M/A-COM, Ireland, and Infineon Technologies, Germany and Austria, as an engineer, researcher, lecturer, and educator. He read lectures as a Guest Professor in University of Linz, Austria, and presented short courses and tutorials as an Invited Speaker at International Microwave Symposium, European and Asia-Pacific Microwave Conferences, and Motorola Design Centre, Malaysia. He is an author of more than 70 papers, 3 books and several European and US patents. He can be reached by grandrei@ieee.org.